AGU PUBLICATIONS

Geophysical Research Letters

RESEARCH LETTER

10.1002/2015GL064457

Key Points:
- Ross Sea bottom water export variability
- Significant seasonal cycle and interannual trend
- Shelf water export regional wind

Correspondence to:
A. L. Gordon,
agordon@ldeo.columbia.edu

Citation:
Gordon, A. L., B. A. Huber, and J. Busecke (2015), Bottom water export from the western Ross Sea, 2007 through 2010, *Geophys. Res. Lett.*, *42*, doi:10.1002/2015GL064457.

Received 5 MAY 2015
Accepted 8 JUN 2015
Accepted article online 10 JUN 2015

Bottom water export from the western Ross Sea, 2007 through 2010

Arnold L. Gordon[1], Bruce A. Huber[1], and Julius Busecke[1]

[1]Lamont-Doherty Earth Observatory of Columbia University, Palisades, New York, USA

Abstract Bottom water export from the Ross Sea, February 2007 to January 2011, exhibits seasonal and interannual variability. Temperature minima coupled to salinity maxima in late austral summer, into the fall, indicate input from High-Salinity Shelf Water (HSSW). Secondary temperature minima lacking the high-salinity trait, characteristic of Low-Salinity Shelf Water (LSSW), appear in the spring. Warmer bottom water similar to modified Circumpolar Deep Water (mCDW) is observed in winter and in early summer. The LSSW and mCDW may be drawn from the Drygalski Basin, as the HSSW pool retreats poleward from the shelf break in response to increased winter polar easterlies allowing these less dense overlying waters to spill into the deep ocean within the benthic layer. Bottom salinity decreased from 2007 to 2011 by 0.007 year^{-1} significantly higher than regional decadal trends, which we propose is a result of HSSW retreat induced by strengthening polar easterlies.

1. Introduction

At several sites along the margin of Antarctica, dense water descends within gravity currents over the continental slope, drawing dense water from the continental shelf, entraining less dense ambient water during descent, and contributing to Antarctic Bottom Water (AABW) [*Legg et al.*, 2009; *Heywood et al.*, 2014]. The Weddell and Ross Seas are the primary sites of export of dense shelf water, with other sites along the Antarctic margins south of Australia and within the Indian Ocean sector [e.g., *Baines and Condie*, 1998; *Legg et al.*, 2009; *Ohshima et al.*, 2013]. Based on chlorofluorocarbon concentrations, the total export of Antarctic shelf water is estimated as 5.4 Sv, which upon entrainment of deep water forms 17.5 Sv of AABW ($1\,\mathrm{Sv} = 10^6\,\mathrm{m}^3\,\mathrm{s}^{-1}$) [*Orsi et al.*, 2001, 2002]. The western Ross Sea is the formation site for a particularly salty variety of AABW [*Gordon*, 1974; *Jacobs et al.*, 1985; *Orsi and Wiederwohl*, 2009] accounting for ~25% of AABW formation [*Orsi et al.*, 2002].

Changes in the global abyssal waters [*Purkey and Johnson*, 2013] as well as observations of the changing stratification on the continental shelf of Antarctica associated with increased glacial melt [*Jacobs and Giulivi*, 2010; *Russo et al.*, 2011; *Rignot et al.*, 2013; *Schmidtko et al.*, 2014] have led to speculations as to how the formation rate and properties of AABW respond to global climate change [*Stewart and Thompson*, 2013, 2015]. To relate changes in AABW formation to climate change forcing requires time series that resolve the seasonal cycle, which is large in comparison to the longer-term trends in many locations, for example, within the Weddell Sea [*Gordon et al.*, 2010] and the Ross Sea [*Bergamasco et al.*, 2003, 2004; *Gordon et al.*, 2004, 2009a; *Budillon et al.*, 2011].

The 2003–2004 Anslope program [*Gordon et al.*, 2009b] and the Climate Long-term Interaction of the Mass balance of Antarctica program [*Budillon et al.*, 2002] observed varied forms of Ross Sea shelf water escaping from the continental shelf descending as a 300–400 m thick gravity current over the continental slope [*Gordon et al.*, 2009a; *Visbeck and Thurnherr*, 2009; *Budillon et al.*, 2011], tending to geostrophic flow at greater depths, eventually leaving the Ross Sea region between the 1500 and 2000 m isobaths off Cape Adare (Figure 1). The most energetic gravity currents observed over the western continental slope of the Ross Sea are relatively salty, as high as 34.82, derived from export of HSSW ($S > 34.7$), much of which is produced by air-sea processes within Terra Nova Polynya [*Fusco et al.*, 2009; *Cappelletti et al.*, 2010; *Rusciano et al.*, 2013]. The Glomar Challenger Basin to the east of Pennell Bank does not enable access of shelf water above 34.72 to the slope, while the Joides Basin offers an escape route for HSSW having an intermediate salinity of up to 34.78 [*Budillon et al.*, 2002, 2011; *Orsi and Wiederwohl*, 2009]. The Anslope 2003–2004 mooring time series [*Gordon et al.*, 2009a] reveal HSSW export (< -1°C; > 34.75) with downslope bottom

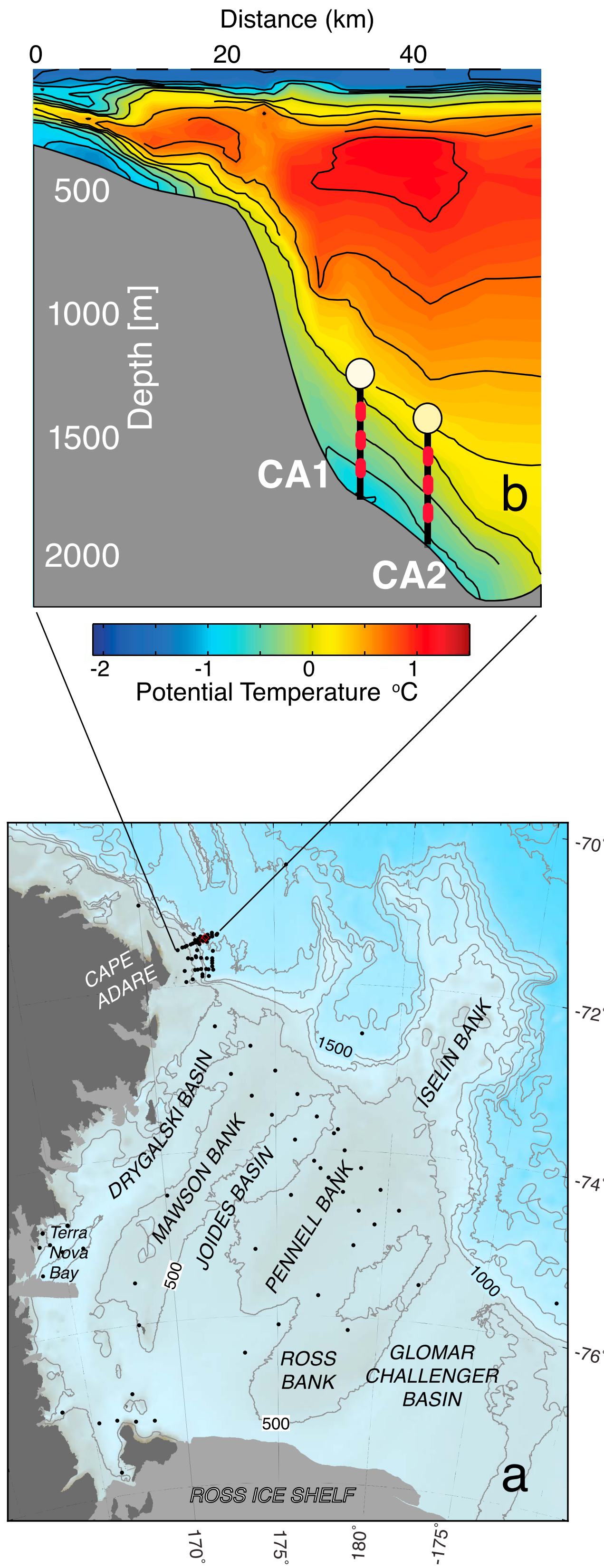

Figure 1. (a) Map of the central and western Ross Sea continental shelf. Feature names follow those in the International Bathymetric Chart of the Southern Ocean (www.ibcso.org); bathymetry from *Smith and Sandwell* [1997]. Contour intervals are 500 m. (b) Potential temperature-depth section across the continental slope near Cape Adare, with the CALM moorings shown schematically. Potential temperature data from Anslope cruise NBP0402.

currents of over 1 $m s^{-1}$, during the austral summer-fall period (December–May), which correlate with northward shifts of the shelf-slope front, as observed by the Anslope moorings over the outer continental shelf.

Cape Adare provides a western boundary pathway for Ross Sea dense water exported from the central and western topographic troughs of the Ross Sea. The northward transport of benthic water observed in austral summer 2004 off Cape Adare was ~1.7 Sv, composed of ~25% HSSW [*Gordon et al.*, 2009a]. Additional export of Ross Sea water into the deep ocean, composed mainly of Low-Salinity Shelf Water (LSSW; including Ice Shelf Water) and modified CirCumpolar Deep Water (mCDW), occurs east of Iselin Bank [*Gordon et al.*, 2009a; *Orsi and Wiederwohl*, 2009].

From January 2008 to January 2011, two moorings, one at 1753 m sea floor depth and the other at 1920 m (Table 1), were deployed off Cape Adare (Cape Adare Long-term Moorings; CALM) to build a time series of the temperature, salinity, and velocity data within the lower 500 m of the water column, for monitoring the export of dense bottom water from the western Ross Sea. In February 2007 to January 2008, a single mooring was deployed at the deeper site. Herein, we present the findings of the CALM time series.

2. Data

The two sites (CA1 and CA2) were instrumented with nearly identical 500 m tall moorings (Table 1). Temperature/pressure (TP) and temperature/conductivity/pressure (TCP) recorders were Sea-Bird

Table 1. Cape Adare Mooring Positions, Period Covered, and Sensor Information[a]

Mooring	Distance Above Bottom (m)	Salinity		Potential Temperature (°C)		Potential Density (Referenced to 1800 dbar; kg/m^3)		Speed (m/s)	
		avg	stdev	avg	stdev	avg	stdev	avg	stdev
CA1-08	476							0.11	0.02
Latitude: −71.4597	460	34.680	0.006	0.224	0.082	1036.227	0.009		
Longitude: 172.3042	298			−0.032	0.101				
Water Depth: 1753 m	175			−0.227	0.115				
Deployed: 1/21/08	43	34.668	0.009	−0.462	0.139	1036.289	0.017		
Recovered: 1/24/11	22							0.27	0.05
CA2-07	470							0.08	0.01
−71.4284	459	34.687	0.003	0.205	0.031	1036.235	0.004		
172.3894	292			−0.096	0.049				
1917 m	*175*	No instrument							
2/5/07	37	34.671	0.009	−0.387	0.066	1036.285	0.011		
1/19/08	34							0.21	0.03
CA2-08	490							0.10	0.01
−71.4270	490	34.684	0.002	0.253	0.044	1036.227	0.004		
172.3850	361			0.071	0.068				
1929 m	207			−0.142	0.092				
1/20/08	41	34.666	0.008	−0.374	0.116	1036.279	0.015		
1/24/11	21							0.23	0.06

[a]avg is record average; std dev is standard deviation.

Electronics models 39 and 37sm, respectively. Current measurements were made with Nortek Aquadopp single-point current meters. Samples were recorded at 30 min intervals then averaged and interpolated to a common hourly time base. TP and TCP recorders were calibrated at the manufacturer following recovery. Differences in predeployment and postdeployment calibrations were interpolated in time before the calibrations were applied to the data. We report only speed for the current measurements; the near bottom current meters experienced frequent large angular displacements from vertical due to energetic tidal excursions that rendered the compass readings unreliable.

The time series data (Figure 2) were smoothed with a third order Butterworth filter with a 30 day cutoff period. Noon-centered daily averages were then computed. Times and dates are GMT. Profiles of salinity, temperature versus depth (conductivity-temperature-depth (CTD)) were obtained near the mooring sites during cruises of the RVIB *Nathaniel B. Palmer* in connection with the CALM program (2007 and 2008). Additional CTD data used in this study were obtained during the Anslope program [*Gordon et al*., 2009a] and during cruise NBP1101 when the moorings were recovered [*Kohut et al*., 2013].

3. CALM Time Series

The CALM time series reveal significant changes of the potential temperature (θ°C) and salinity characteristics of the northward flowing bottom water off Cape Adare (Figures 2 and 3 and Table 1). Seasonal fluctuations are clearly evident (Figure 2a), as are year-to-year changes. The fluctuations at both sites are intensified as the sea floor is approached, as expected in a flow originating from a gravity current [*Legg et al*., 2009].

3.1. Seasonal Signal

At CA1 for the period 21 January 2008 to 24 January 2011, the bottom θ (43 m above the sea floor) averaged −0.462°C, with a standard deviation of 0.139°C. At 460 m above the sea floor, the corresponding values are 0.224°C and 0.082°C: the near bottom θ is 0.686°C colder, with a seasonal oscillation of almost twice that observed 460 m above the sea floor. At the deeper CA2 site (2008–2011 period corresponding to the CA1 record), the bottom θ at 41 m above the sea floor is 0.1°C warmer, with a more subdued seasonal signal than that observed at CA1, suggesting that the core of the gravity current has not yet descended to 1920 m.

The salinity near the sea floor is slightly fresher (0.012 and 0.018) than that recorded near 460 and 490 m above the sea floor at CA1 and CA2, respectively, but notable is the larger seasonal signal near the sea floor, often with bottom salinity exceeding that at 460 and 490 m, an indicator of increased HSSW-derived

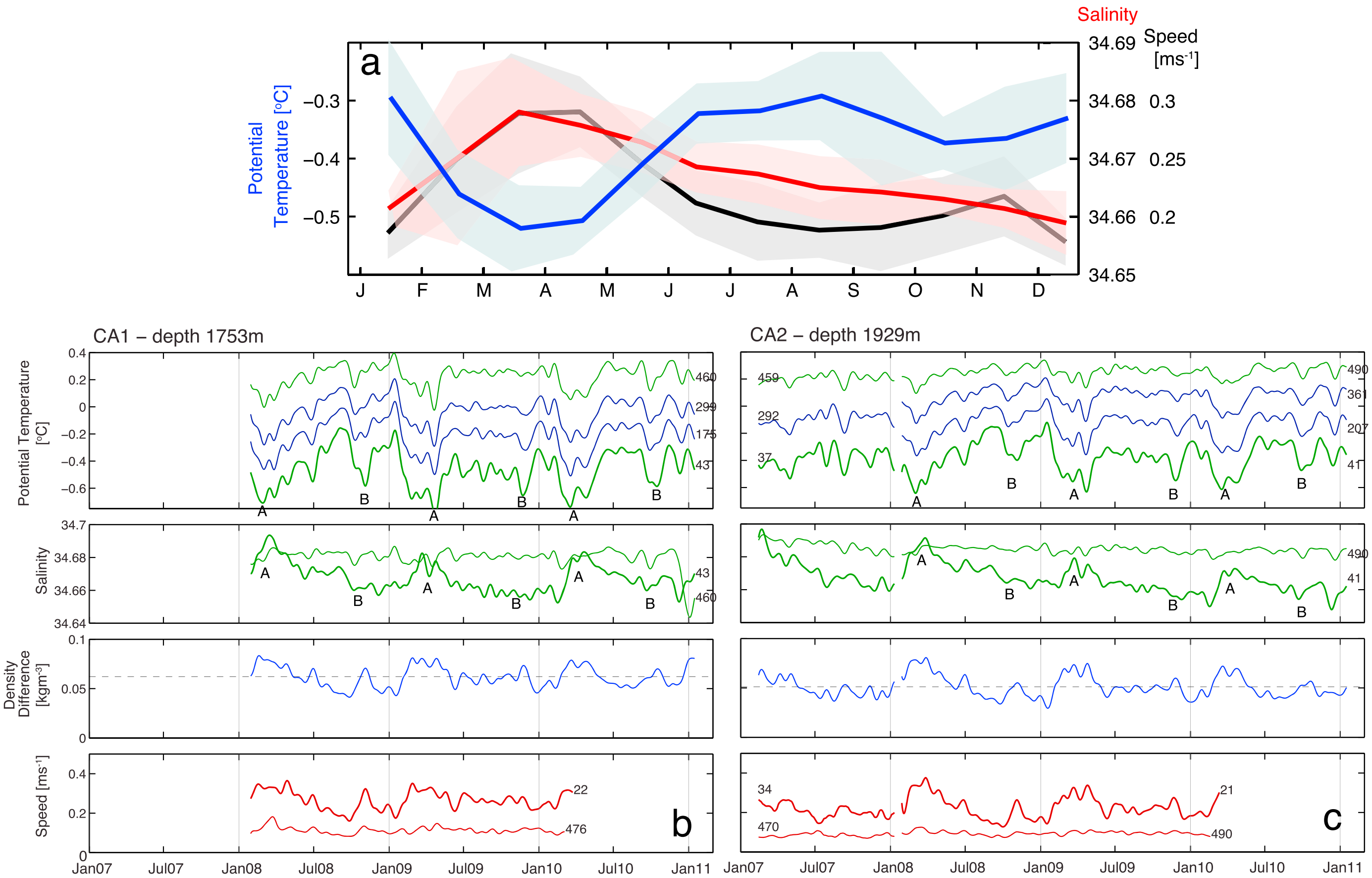

Figure 2. (a) Monthly averaged potential temperature (blue), salinity (red), and speed (black) for the near bottom sensors at site CA2. Shaded envelopes are ±1 standard deviation. (b and c) Time series of potential temperature, salinity, and of the density difference and speed of the deepest and shallowest sensor, from mooring CA1 and CA2, smoothed with a low-pass Butterworth filter with a 30 day cutoff period. The numbers associated with each line represent the distance (meters) from the sea floor. A and B refer to two types of cold events observed in the time series, also shown in Figure 3. The mean difference of potential density (referenced to 1800 dbar) is represented by the dashed horizontal lines on the plots.

bottom water. The mean potential density difference (referenced to pressure of 1800 dbar, $\sigma_{1.8}$, so as to incorporate the thermobaric effect) [*Gordon et al.*, 2009a] for CA1 is 0.062 kg/m^3, while that for CA2 is 0.051.

The speed increases as the sea floor is approached. The shear from 476 m to 22 m above the sea floor at CA1 and from 490 m and 21 m at CA2 is d*v*/d*z* of 3.37×10^{-4} and 2.81×10^{-4} m^2 s^{-1}, respectively; the larger shear at CA1 reflects the greater $d\theta/dz$ and $d\sigma/dz$ relative to CA2.

At both sites, the sea floor temperature minimum (θ min) coincides with a salinity maximum (*S* max; marked by "A" in Figures 2 and 3), indicating an increase of the cold saline HSSW, during February–May, late austral summer into the fall season. The mean bottom current speed at the time of the θ min/*S* max attains maximum values of approximately 0.35 to 0.40 ms^{-1} at CA2 and 0.25 to 0.30 m/s at CA1 (Figures 2 and 3b). A characteristic bottom speed of 0.3 ms^{-1} from the northern entrance to Drygalski Basin to the CALM sites (consistent with the Anslope results) [*Gordon et al.*, 2009a] indicates that the export of HSSW occurs only days before reaching the CALM sites.

The seasonality of HSSW export is likely related to the polar easterlies (wind from east to west) along the outer shelf [*Gordon et al.*, 2009a; *Stewart and Thompson*, 2013], which are markedly stronger during the austral winter months, receding to a minimum in February–April months (Figure 4). Northward shift of the leading edge of the dense shelf water (the shelf front) toward the continental slope occurs as the easterly wind diminishes, as observed during the Anslope program (Figure 12 of *Gordon et al.* [2009a] records reduced salinity of the bottom water over the outer shelf during the winter, as the HSSW retreats poleward), providing access of the HSSW to the continental slope; we infer that stronger polar easterlies shift the

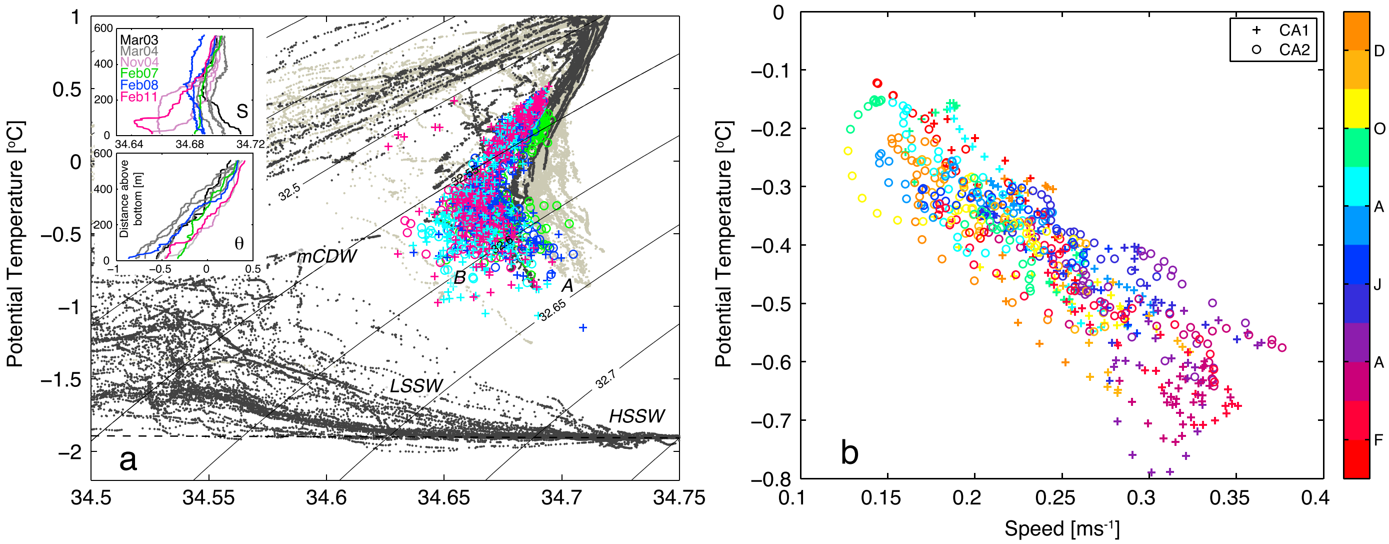

Figure 3. (a) Potential temperature/salinity (θ/S) scatterplot from CA1 (cross) and CA2 (circle). Data shown are daily averages, plotted every third day. Color of symbol indicates year of data collection: 2007, green; 2008, blue; 2009, aqua; and 2010, magenta, superimposed on θ/S from CTD stations taken in the Cape Adare region during 2003 and 2004 Anslope (brown) and RVIB *Nathaniel B. Palmer* stations (black) obtained in 2007, 2008, and 2011. Density contours are sigma 1000. Salinity and θ profiles, same year color code as the θ/S, collected in vicinity of mooring plotted as distance in meters off the sea floor are shown in the insert. The approximate θ/S end-member characteristics are marked: HSSW, High-Salinity Shelf Water; LSSW, Low-Salinity Shelf Water; mCDW, Modified Circumpolar Deep Water; and A and B refer to cold events, as shown in Figure 2b. (b) Daily average of 30 day low-pass filtered potential temperature versus speed for near bottom sensors. Every third day is plotted for clarity of presentation. Data are color coded by month. Correlation coefficients for CA1 and CA2 are −0.87 and −0.84, respectively, with 95% confidence intervals of +0.02 and −0.01 for both.

front poleward, reducing HSSW export to the slope. This is similar to observations in the western Weddell Sea [*McKee et al*., 2011]. *Budillon et al*. [2011] report that a time series at the shelf break sea floor of Drygalski Basin reveals saltier HSSW in March–May 2005, indicating it was shifted farther north, with minimum salinity in October–November 2004 and September–November 2005, consistent with the Anslope results and CALM time series. In early 2004, the HSSW shelf water was anomalously salty. The polar easterlies were at a minimum in 2004 (Figure 4), which may have induced a more northern shift of the HSSW. The release of the dense shelf water to the deep ocean that occurs in late summer-early fall months is out of phase with the formation of the dense shelf water, which is associated with winter air-sea forcing.

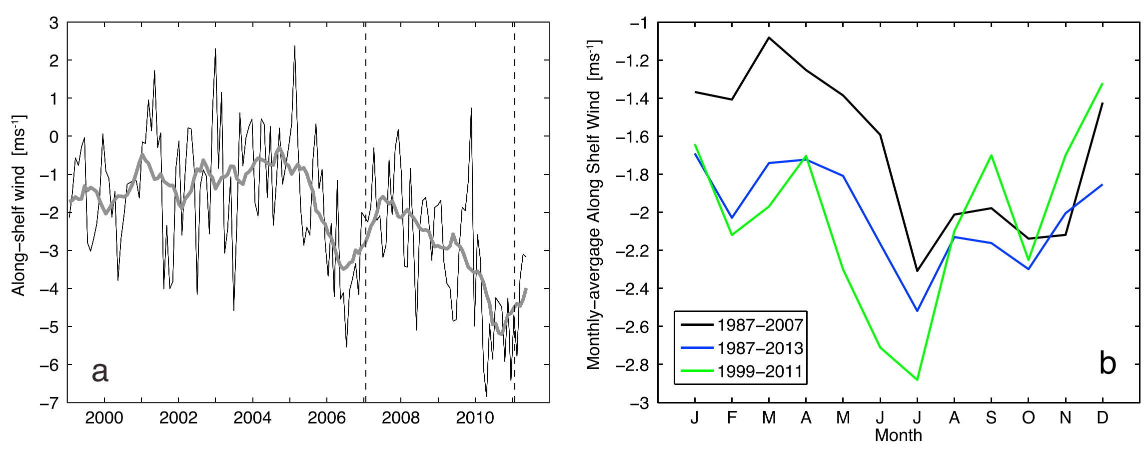

Figure 4. (a) Along-shelf monthly wind (black line) with 13 month running mean (gray line) averaged within the box 70°–75°S, 175°E to 175°W; negative values represent wind directed toward the west. Dashed lines mark the beginning and end of CALM mooring period. (b) Climatology of monthly along-shelf wind in the same area as Figure 4a computed for the three epochs indicated. Along-shelf wind is obtained by rotating the coordinate system by 40° so that U roughly aligns with the Ross Sea shelf break at 175 W. Monthly wind are obtained from the CDAS product (Climate Data Assimilation System at NOAA National Centers for Environmental Prediction/National Center for Atmospheric Research Reanalysis Project) accessed 14 October 2014 from http://iridl.ldeo.columbia.edu/SOURCES/.NOAA/.NCEP-NCAR/.CDAS-1/.MONTHLY.

A secondary θ min is observed at both sites in the austral spring, October–November (marked by "B" in Figures 2 and 3), lacking the relatively high salinity characteristic of HSSW. It likely marks the presence of LSSW that overlies the HSSW (Figure 3). The θ and S profiles (Figure 3 insert) observed by CTD stations near the CALM sites reveal a S min ~100–300 m off the sea floor, except for the two profiles in November 2004 when the bottom water is cold and relatively fresh, consistent with water type B as observed by the CALM time series. The S min of the CALM time series closer to the sea floor is colder, matching LSSW characteristics, while the warmer S min farther from the sea floor is closer to mCDW characteristics. The February 2011 CTD profile reveals low-bottom water salinity, with a S min about 80 m above the sea floor, but as pointed out in the "interannual signal" discussion below, the bottom water becomes increasingly lower in salinity during the CALM time series, a consequence, we propose below, of strengthening polar easterlies.

The geographic source of the LSSW is not resolved by the CALM time series. If the source of the LSSW observed at the CALM mooring were Glomar Challenger Basin, using the 0.3 m s^{-1} bottom speed suggests the time of export is ~1 month prior to its presence at the CALM site, e.g., September–October. However, this is the time of strong polar easterlies (Figure 4) when the shelf front is shifted poleward potentially reducing the LSSW access to the deep ocean. A more plausible scenario is that as the HSSW within Drygalski Basin retreats poleward during the strong polar easterlies of the winter/spring season, enabling the LSSW that caps the HSSW to approach the sea floor at the shelf break, resulting in export to the deep ocean within the benthic Ekman layer [*Meredith et al.*, 2011]. In this scenario, the LSSW export occurred just days before reaching the CALM moorings, as does the HSSW signal recorded at the CALM moorings in the late summer.

A relatively warm (−0.3°C) bottom water is observed in August. The θ/S properties of this water suggest a mCDW source (Figure 3). As the mCDW is less dense than the LSSW, this implies a large poleward shift of the shelf-slope front, when even LSSW has limited access to the continental slope. The strongest polar easterlies occur in July, consistent with this concept. Relatively warm bottom water is also observed in January and may not be drawn from the local Drygalski Basin but rather from a more remote region to the east where mCDW has a greater presence and is exported to the deep ocean [*Orsi and Wiederwohl*, 2009], which implies that at times, mCDW curls around the northern rim of Iselin Bank toward Cape Adare.

3.2. Interannual Signal

In addition to the seasonal signal, trends are also evident across the span of the time series (Figures 2 and 3). At CA2, the bottom salinity maximum decreased from 2007 to 2010 by 0.007 year^{-1}. At CA1, the bottom salinity also decreases but at a rate slightly smaller than at CA2. As CA1 is only a 3 year record versus the 4 years of CA2, the difference may not be significant. *Budillon et al.* [2011] find freshening of the HSSW based on four ship-based realizations (a fifth realization in 2003 displayed high-HSSW salinity is tagged as anomalous because of the C-19 iceberg presence) at the shelf break of Drygalski Basin of 0.06 over an 11 year period (1995–2006) or 0.005 year^{-1}, which is close to the freshening observed at the CALM site.

The θ/S scatter (Figure 3) further illustrates the trends of the bottom water salinity. The salinity within the −0.2 to −0.5°C range generally represents the salinity minimum within the 500 m benthic layer measured. Below the local S min, there is an increasing presence of HSSW (A); at warmer temperatures there is increasing concentration of mCDW. From 2007 to 2010, HSSW effect decreases. None of the CALM data points attain as high salinity as observed in the Anslope data, a possible consequence of strong HSSW export attributed to the presence of a grounded large iceberg, C-19 in the Drygalski Basin region [*Gordon et al.*, 2009a]. An additional factor may be the weak polar easterlies in 2003–2004, which would lead to a release of HSSW into the gravity currents over the slope.

The 2007 to 2011 decrease of bottom salinity at CA2 was approximately 10 times larger than decadal trends of salinity of the lower 600 m of 1500–2500 m water depths of the northwest Ross Sea, of 0.0006 to 0.0008 year^{-1}, as reported by *Jacobs and Giulivi* [2010]. While the decadal freshening of bottom water may be a contributing factor, it is not the primary reason for the decreasing bottom salinity observed over the 4 years CALM time series. It is more likely that the decreased HSSW presence at the CALM moorings is a result of reduced HSSW export due to changes in the polar easterlies, which increased in strength during the CALM mooring time series. The HSSW at the CALM moorings from 2007/08 to 2009/10 (Figure 3) is replaced by more frequent LSSW and mCDW events, a consequence of the poleward shift of the shelf front, limiting HSSW export.

4. Conclusions

The CALM moored data set represents nearly continuous observations of the outflow of AABW generated within the western Ross Sea over 4 years from 2007 through 2010. The length of the time series allows resolution of the seasonal variability and reveals interannual changes. The maximum bottom speeds, at the time of the coldest and saltiest events marking a HSSW source, occur in late austral summer into the fall season. Late summer export of Weddell shelf water has also been reported for the Weddell Sea [*Gordon et al*., 2010; *McKee et al*., 2011]. A secondary cold bottom water event, not coupled to high salinity, is recorded in October–November, suggesting a LSSW origin. The warmest, freshest bottom water occurs in both January and July periods, representing the presence of mCDW at the sea floor. We attribute the seasonality of the bottom water reaching the CALM moorings to the seasonal cycle in the polar easterlies.

A decline in salinity over the 4 year CALM time series is evident. However, the trend is 10 times that of the decadal regional salinity decrease of HSSW, and a more local, dynamic effect is suggested: reduced contribution of western Ross Sea HSSW by strengthening of the polar easterlies.

Consistent with the results of *Stewart and Thompson* [2012, 2013, 2015] and overview presented by *Heywood et al*. [2014], we find that the magnitude of the polar easterlies along the shelf break is an important factor in governing the shelf water exported within the Ekman benthic layer into the continental shelf gravity currents. Increased polar easterlies shift the densest shelf water, HSSW, poleward allowing less dense shelf water, e.g., LSSW and mCDW, to feed into the gravity currents. We speculate that the role of Antarctica's margins to deep ocean overturning in our future climate is dependent not only on the air-sea buoyancy flux but also on the strength of the polar easterlies, as suggested by the model based research of *Stewart and Thompson* [2012, 2013].

Acknowledgments
This work was supported by NSF-OPP ANT 0538148 and NSF-OPP ANT 1141890. M. Visbeck is acknowledged with gratitude for his participation in the early stages of developing the CALM project. Lamont-Doherty Earth Observatory contribution 7907. The CTD and mooring time series data used in the paper are available upon request to the authors and from the URLs http://www.marine-geo.org/tools/search/entry.php?id=NBP0801 and http://www.marine-geo.org/tools/search/entry.php?id=NBP1101.

The Editor thanks two anonymous reviewers for their assistance in evaluating this paper.

References

Baines, P. G., and S. Condie (1998), Observations and modeling of Antarctic downslope flows: A review, in *Oce, Ice, and Atm: Interactions at the Ant Cont. Margin*, *Ant. Res. Ser*., vol. 75, edited by S. Jacobs and R. Weiss, pp. 29–49, AGU, Washington, D. C.

Bergamasco, A., V. Defendi, E. Zambianchi, and G. Spezie (2003), Evidence of dense water overflow on the Ross Sea shelf-break, *Antarct. Sci.*, *14*(03), 271–277, doi:10.1017/S0954102002000068.

Bergamasco, A., V. Defendi, G. Budillon, and G. Spezie (2004), Downslope flow observations near Cape Adare shelf-break, *Antarct. Sci.*, *16*, 199–204, doi:10.1017/S0954102004001981.

Budillon, G., S. G. Cordero, and E. Salusti (2002), On the dense water spreading off the Ross Sea shelf (Southern Ocean), *J. Mar. Syst.*, *35*, 207–227.

Budillon, G., P. Castagno, S. Aliani, G. Spezie, and L. Padman (2011), Thermohaline variability and Antarctic bottom water formation at the Ross Sea shelf break, *Deep Sea Res.*, *58*(10), 1002–1018, doi:10.1016/j.dsr.2011.07.002.

Cappelletti, A., P. Picco, and T. Peluso (2010), Upper ocean layer dynamics and response to atmospheric forcing in the Terra Nova Bay polynya, Antarctica, *Antarct. Sci.*, *22*(03), 319–329, doi:10.1017/S095410201000009X.

Fusco, G., G. Budillon, and G. Spezie (2009), Surface heat fluxes and thermohaline variability in the Ross Sea and in Terra Nova Bay Polynya, *Cont. Shelf Res.*, *29*(15), 1887–1895, doi:10.1016/j.csr.2009.07.006.

Gordon, A. L. (1974), Varieties and variability of Antarctic bottom water, in *Processus de Formation des Eaux Oceaniques Profondes (en particulier en Mediterranee Occidentale)*, vol. 215, pp. 33–47, Editions du Centre National de la Recherche Scientifique, Paris, France.

Gordon, A. L., E. Zambianchi, A. Orsi, M. Visbeck, C. F. Giulivi, T. Whitworth III, and G. Spezie (2004), Energetic plumes over the western Ross Sea continental slope, *Geophys. Res. Lett.*, *31*, L21302, doi:10.1029/2004GL020785.

Gordon, A. L., A. H. Orsi, R. Muench, B. A. Huber, E. Zambianchi, and M. Visbeck (2009a), Western Ross Sea continental slope gravity currents, *Deep Sea Res., Part II*, *56*, 796–817, doi:10.1016/j.dsr2.2008.10.037.

Gordon, A. L., A. Bergamasco, and L. Padman (2009b), Southern ocean shelf slope exchange, *Deep Sea Res., Part II*, *56*(13–14), 775–777.

Gordon, A. L., B. A. Huber, D. McKee, and M. H. Visbeck (2010), A seasonal cycle in the export of bottom water from the Weddell Sea, *Nat. Geosci.*, *3*, 551–556, doi:10.1038/ngeo916.

Heywood, K. J., et al. (2014), Ocean processes at the Antarctic continental slope, *Phil. Trans. R. Soc. A*, *372*, doi:10.1098/rsta.2013.0047.

Jacobs, S. S., and C. F. Giulivi (2010), Large multidecadal salinity trends near the Pacific–Antarctic Continental Margin, *J. Clim.*, *23*, 4508–4524.

Jacobs, S. S., R. G. Fairbanks, and Y. Horibe (1985), Origin and evolution of water masses near the Antarctic continental margin: Evidence from $H_2{}^{18}O/H_2{}^{16}O$ ratios in seawater, in *Oceanology of the Antarctic Continental Shelf, Antarct. Res. Ser.*, vol. 43, edited by S. S. Jacobs, pp. 59–85, AGU, Washington, D. C., doi:10.1029/AR043p0059.

Kohut, J., E. Hunter, and B. Huber (2013), Small-scale variability of the cross-shelf flow over the outer shelf of the Ross Sea, *J. Geophys. Res. Oceans*, *118*, 1863–1876, doi:10.1002/jgrc.20090.

Legg, S., et al. (2009), Improving oceanic overflow representation in climate models: The Gravity Current Entrainment Climate Process Team, *Bull. Am. Meteorol. Soc.*, *90*(5), 657–670.

McKee, D., X. Yuan, A. L. Gordon, B. A. Huber, and Z. Dong (2011), Climate impact on interannual variability of Weddell Sea bottom water, *J. Geophys. Res.*, *116*, C05020, doi:10.1029/2010JC006484.

Meredith, M. P., A. L. Gordon, A. C. Naveira Garabato, E. P. Abrahamsen, B. A. Huber, L. Jullion, and H. J. Venables (2011), Synchronous intensification and warming of Antarctic Bottom Water outflow from the Weddell Gyre, *Geophys. Res. Lett.*, *38*, L03603, doi:10.1029/2010GL046265.

Ohshima, K. I., et al. (2013), Antarctic Bottom Water production by intense sea-ice formation in the Cape Darnley Polynya, *Nat. Geosci.*, *6*, 235–240, doi:10.1038/NGEO1738.

Orsi, A. H., and C. L. Wiederwohl (2009), A recount of Ross Sea waters, *Deep Sea Res., Part II*, *56*(13–14), 778–795, doi:10.1016/j.dsr2.2008.10.033.

Orsi, A. H., S. S. Jacobs, A. L. Gordon, and M. Visbeck (2001), Cooling and ventilating the Abyssal Ocean, *Geophys. Res. Lett.*, *28*(15), 2923–2926, doi:10.1029/2001GL012830.

Orsi, A., W. Smethie, and J. Bullister (2002), On the total input of Antarctic waters to the deep ocean: A preliminary estimate from chlorofluorocarbon measurements, *J. Geophys. Res.*, *107*(C8), 3122, doi:10.1029/2001JC000976.

Purkey, S., and G. Johnson (2013), Antarctic bottom water warming and freshening: Contributions to sea level rise, ocean freshwater budgets, and global heat gain, *J. Clim.*, *26*, 6105–6122.

Rignot, E., S. Jacobs, J. Mouginot, and B. Scheuchl (2013), Ice-shelf melting around Antarctica, *Science*, *341*(6143), 266–270, doi:10.1126/science.1235798.

Rusciano, E., G. Budillon, G. Fusco, and G. Spezie (2013), Evidence of atmosphere-sea ice-ocean coupling in the Terra Nova Bay polynya (Ross Sea-Antarctica), *Cont. Shelf Res.*, *61–62*, 112–124.

Russo, A., A. Bergamasco, S. Carniel, L. Grieco, M. Sclavo, and G. Spezie (2011), Climatology and decadal variability of the Ross Sea shelf water, *Adv. Oceanogr. Limnol.*, *2*(1), 55–77, doi:10.1080/19475721.2011.575179.

Schmidtko, S., K. J. Heywood, A. F. Thompson, and S. Aoki (2014), Multidecadal warming of Antarctic waters, *Science*, *346*(6214), 1227–1231, doi:10.1126/science.1256117.

Smith, W. H. F., and D. T. Sandwell (1997), Global seafloor topography from satellite altimetry and ship depth soundings, *Science*, *277*, 1957–1962, doi:10.1126/science.277.5334.1956.

Stewart, A. L., and A. F. Thompson (2012), Sensitivity of the ocean's deep overturning circulation to easterly Antarctic winds, *Geophys. Res. Lett.*, *39*, L18604, doi:10.1029/2012GL053099.

Stewart, A. L., and A. F. Thompson (2013), Connecting Antarctic cross-slope exchange with Southern Ocean overturning, *J. Phys. Oceanogr.*, *43*, 1453–1471.

Stewart, A. L., and A. F. Thompson (2015), Eddy-mediated transport of warm Circumpolar Deep Water across the Antarctic shelf break, *Geophys. Res. Lett.*, *42*, 432–440, doi:10.1002/grl.v42.2.

Visbeck, M., and A. M. Thurnherr (2009), High-resolution velocity and hydrographic observations of the Drygalski trough gravity plume, *Deep Sea Res., Part II*, *56*(13–14), 835–842, doi:10.1016/j.dsr2.2008.10.029.